

Change in spectra of mobility of small atmospheric ions during convection and diffusion

Toshiro Maruyama^{a)} and Makoto Wakabayashi

Department of Chemical Engineering, Graduate School of Engineering, Kyoto University,
Kyoto 615-8510, Japan

(Received 23 September 2004; accepted 27 September 2005; published online 11 November 2005)

The change in spectra of mobility of small atmospheric ions during molecular diffusion and convection in air has been studied experimentally. There occurs no change in mobility spectra for the molecular diffusion in windless air because both coefficients of adhesion and diffusion are proportional to the mobility. On the other hand, the mobility spectrum of ions changes during the convections due to the inverse proportionality of the lifetime to the mobility of ions. The mean lifetime of ions was experimentally obtained from the measured concentration distribution of ions in a round free jet. The results showed that the mobility spectrum of ions changes with increasing downstream distance due to a rapid dissipation of the ions of high mobility during the convections. © 2005 American Institute of Physics. [DOI: 10.1063/1.2127123]

I. INTRODUCTION

Charged small particles floating in air are called atmospheric ions, which are classified into small ions and large ions.¹ The small ions are unit charged cluster ions, the diameter being an order of 1 nm. On the other hand, the range of diameter of large ion extends to that of the aerosol (from 10 nm to 10 μm). The large ions of large diameter sometimes have multiple charges.

The electrical structure of the lower atmosphere has been studied by many researchers.^{2,3} A pair of small ions is formed at a rate¹ of $10\text{ cm}^{-3}\text{ s}^{-1}$ by the ionization of air molecules due to natural mechanisms, e.g., cosmic rays, ground radioactivity, and radioactive decay of radon, thoron, and their derivatives which are given off by the ground and mix with the atmosphere.⁴ The generated small ions diffuse and immediately react with surrounding molecules, combine with water molecules,⁵ and become various chemical species⁶ of a wide range of mobility. The dynamic behavior of the spectrum of the mobility of the small ions depends on the coordination number and chemical species. Nagato and Ogawa^{5,6} and Nagato⁷ have measured the dynamics of the mobility spectra with draft-tube-type ion mobility spectrometer. They reported that the spectrum of the mobility of the small ions develops within a few seconds after the generation.⁵ It develops not only to a lower mobility but also to a higher mobility, forming a spectrum of a wide range of mobility.⁶ There is a large difference in spectrum of the mobility between positive and negative ions, suggesting the large difference in reaction paths.⁷ However, the natural mobility spectra of negative and positive small ions reported by various researchers are not so different with each other. For example, Hörrak *et al.*¹ described that the general shapes of the mobility spectra of negative and positive small ions in pure atmosphere (N_2 , O_2 , CO_2 , and H_2O) are astonishingly similar to those observed by Misaki.⁸

The lifetimes of the small ions end by the adhesion to another particle. When the small ions collide with aerosol particles and attach to them, they form the charged aerosols. The mean time interval between the generation of a small ion and its attachment to another particle is relatively short. Briard and Pradel⁴ described the value of the mean lifetime as 30–50 s under normal conditions. Recently, one of the authors⁹ reported that the mean lifetime of small negative ions in air was 30 s on the basis of the measured concentration of the ions convectively transferred by a free round jet. However, it is questionable that the behavior of the small ion can be treated by using the mean value for each characteristics, because of the wide range of mobility.

Small negative atmospheric ions have attracted attention because the application of ions to the human body is inferred to have prominent effects on physiological reactions. Recently, various kinds of artificial generators of small atmospheric negative ions have been used to compensate for the decrease of natural ions in a house. The ions generated are transported to the human body by diffusion and convection in air. This article deals with the behavior of artificially generated small atmospheric ions during molecular diffusion and convection in air, by analyzing the behavior of the component of a narrow range of mobility. The change in spectrum of the mobility is discussed by comparing analysis with measured variations of the concentration and mean lifetime of small ions, which are artificially produced in the ambient air near the ground.

II. LIFETIME OF SMALL IONS IN AIR

The temporal variations of the concentration n of small ions in air are expressed as

$$dn_+/dt = q - \alpha n_+ n_- - \eta_{+0} n_+ N_0 - \eta_{+-} n_+ N_-, \quad (1)$$

$$dn_-/dt = q - \alpha n_+ n_- - \eta_{-0} n_- N_0 - \eta_{-+} n_- N_+, \quad (2)$$

where N represents the concentration of large particles. Subscripts +, -, and 0 refer to positive, negative, and neutral

^{a)} Author to whom correspondence should be addressed; electronic mail: maruyama@cheme.kyoto-u.ac.jp

electric charges, respectively. α represents the coefficient of recombination of small ions with ions of opposite sign, and η is the coefficient of adhesion of small ions to particles (aerosol). The first term on the right-hand side, q , expresses the generation rate of an ion pair, the second term dissipation by the recombination of small ions, and the third and fourth terms dissipation of the small ions upon adhesion to large neutral and opposite-sign particles, respectively.

If we assume that $n_+ = n_-$ and that the mobility of a negative ion is equal to that of a positive ion, Eqs. (1) and (2) can be approximated by

$$dn/dt = q - \alpha n^2 - 2\eta_+ n_+ N_- = q - \alpha n^2 - \beta n N. \quad (3)$$

An estimate^{10,11} for application to the atmosphere on land shows that $n = 10^8 \text{ m}^{-3}$, $N = 10^{10} \text{ m}^{-3}$, and α and $\beta = 10^{-12} \text{ m}^3 \text{ s}^{-1}$. Therefore, Eq. (3) can be further approximated by

$$dn/dt = q - \beta n N. \quad (4)$$

When generation is stopped, i.e., $q=0$, the concentration of ions after t in seconds is expressed as

$$n = n_0 \exp(-\beta N t). \quad (5)$$

The lifetime of ions τ is defined as

$$\tau = 1/\beta N = 1/2 \eta N. \quad (6)$$

According to Bricard,^{12,13} the coefficient of adhesion of small ions to aerosol η is expressed as

$$\eta = 4\pi Da \int_1^\infty x^{-2} \exp\{(e\mu/Da)(p/x) - (1/2)x^2(x^2 - 1)\} dx, \quad (7)$$

where D represents the diffusion coefficient, a is the diameter of aerosol, e is the elementary charge, p is the multiplication number of the elementary charge, and μ is the mobility. In the meantime, Einstein equation shows that the diffusion coefficient is proportional to the mobility

$$D = k_B T \mu / e, \quad (8)$$

where k_B represents the Boltzmann constant and T is the absolute temperature. Therefore the lifetime is inversely proportional to the mobility.

III. MOBILITY SPECTRUM

Figure 1 shows the mobility spectra of small air ion measured in natural atmosphere by Misaki.⁸ Apparently the mobility shows a wide range of value. Therefore the lifetime should have a wide range of value, and there should be changes in spectra in nonequilibrium conditions. We study the changes in spectra in three nonequilibrium conditions, i.e., (i) molecular diffusion in windless air, (ii) convection by a free round jet, and (iii) convection in a human body by breathing, under the assumptions that the mobility spectra at the origin of jet are those in equilibrium condition, because the required time to develop spectra is within a few seconds and consequently, negligibly small compared to the mean lifetime (30–50 s).

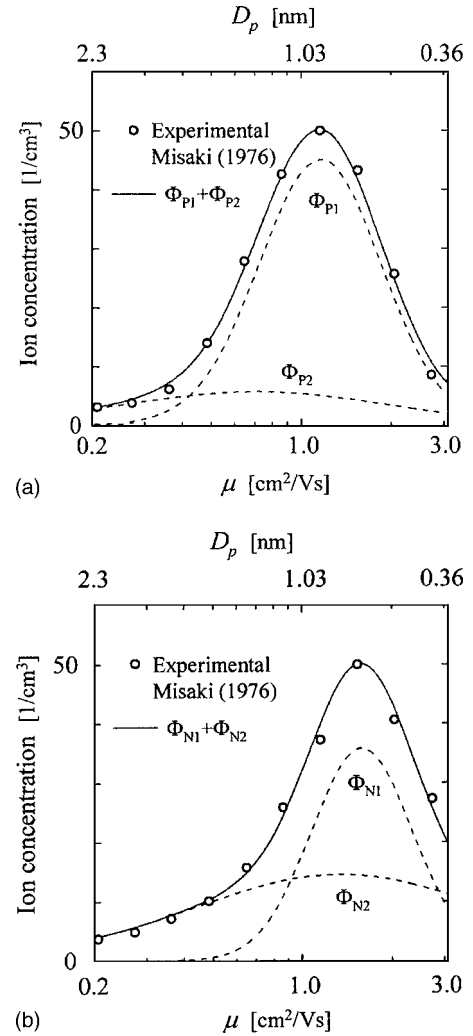


FIG. 1. Mobility spectra of small (a) positive and (b) negative atmospheric ions measured in natural atmosphere by Misaki (see Ref. 8).

In the analysis, each mobility spectra in equilibrium condition is expressed by a combination of two logarithmically normal distribution:¹⁴ ϕ_{N1} [mean value $E(\mu)=3.603$ and dispersion $V(\mu)=0.382$] and ϕ_{N2} [$E(\mu)=6.196$ and $V(\mu)=10.91$] for negative ion, and ϕ_{P1} [$E(\mu)=3.251$ and $V(\mu)=0.445$] and ϕ_{P2} [$E(\mu)=4.059$ and $V(\mu)=3.648$] for positive ion. These distributions and their compositions are shown in Fig. 1. The compositions well represent the measured distributions.

IV. DIFFUSION OF SMALL IONS IN WINDLESS AIR

Under most conditions where carrier diffusion in gases is considered, the electrostatic forces between individual carriers can be neglected.¹⁵ The basic equation of diffusion of i component of small ions with dissipation by collision with large particles is expressed as¹⁶

$$(1/r^2)d(r^2 D_i dn_i/dr)/dr = \beta_i n_i N, \quad (9)$$

where D_i and β_i , respectively, represents the diffusion coefficient and β of the i component of small ion, and r the radial distance from the source. The boundary conditions are

$$n_i = n_{i0} \quad \text{at } r = r_0, \quad (10)$$

$$n_i = 0 \quad \text{at } r = \infty. \quad (11)$$

The solution is expressed with two dimensionless combined variables, $r_0(\beta_i N/D_i)^{1/2}$ and r/r_0 , as

$$n_i/n_{i0} = \exp[-r_0(\beta_i N/D_i)^{1/2}(r/r_0 - 1)]/(r/r_0). \quad (12)$$

In this equation, β_i/D_i is constant because both β_i and D_i are proportional to the mobility μ_i [see Eqs. (7) and (8)].

Therefore

$$n_1/n_{10} = n_2/n_{20} = \dots = n_i/n_{i0}. \quad (13)$$

Thus the proportionality to the initial concentration n_{i0} persists in spectra during the diffusion, and consequently the small ions diffuse in windless air with keeping the similar spectrum of the mobility.

V. CONVECTIVE TRANSFER OF SMALL IONS BY A FREE ROUND JET

A. Analysis

The basic equation of convection of i component of small ions with dissipation by collision with large particles is expressed as¹⁶

$$U_j \partial n_i / \partial r + V_j \partial n_i / \partial z = -\beta_i n_i N, \quad (14)$$

where U_j and V_j represent the radial and axial components of the velocity of the jet and z the axial distance. Multiplication by $2\pi r$ and an integration from $r=0$ to $r \rightarrow \infty$ yield

$$\begin{aligned} \int_0^\infty 2\pi r U_j (\partial n_i / \partial r) dr + \int_0^\infty 2\pi r V_j (\partial n_i / \partial z) dz \\ = -\beta_i N \int_0^\infty 2\pi r n_i dr. \end{aligned} \quad (15)$$

For simplicity in calculation, the velocity V_j and concentration n_i in the cross section of the jet are approximated as constant, that is, it is assumed that $V_j = V_j(z)$ and $n_i = n_i(z)$. By applying the equation of continuity the first term of the left-hand side of Eq. (15) can be expressed as $n_i(\partial Q_j / \partial z)$ and consequently, Eq. (15) is expressed in simple form as

$$d(Q_j n_i) / dz = -\beta_i n_i N A_j, \quad (16)$$

where Q_j represents the volumetric flow rate of the jet and A_j is the cross-sectional area of the jet.

The concentration n_i at z is given by

$$n_i/n_{i0} = \exp\left[-\int_0^z (A_j \beta_i N + E)/(Q_j + E) dz\right], \quad (17)$$

where E is the entrainment of jet. For changes of the radius and mean velocity of the jet with z , the law of the conservation of momentum is assumed

$$Q_i V_j = Q_{i0} V_{j0}. \quad (18)$$

The diameter¹⁷ of the jet at z is given by

$$d_j = d_{j0} + 2z \tan(\theta/2), \quad (19)$$

where $\theta = 14^\circ$.

The mean lifetime τ_{ave} is defined by Eq. (20)

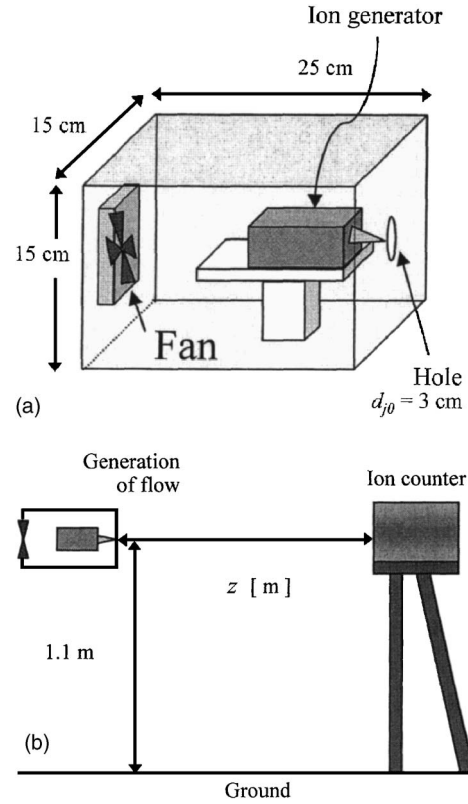


FIG. 2. Schematic representations of (a) chamber of generator and (b) experimental setup.

$$\tau_{\text{ave}} = 1/\beta_{\text{ave}} N, \quad (20)$$

where

$$\beta_{\text{ave}} = \sum_i n_i \beta_i / n. \quad (21)$$

Accordingly, τ_{ave} can be obtained from the overall material balance

$$d(Q_j n) / dz = -\beta_{\text{ave}} n N A_j, \quad (22)$$

as

$$\tau_{\text{ave}} = -(A_j n) / [d(Q_j n) / dz]. \quad (23)$$

B. Experiment

The concentration distributions of small ions in air were measured along a free round jet. Figure 2 shows the schematic representations of the experimental apparatus. A dc corona discharge was used as the ion generator. The chamber of the generator had inner dimensions of $15 \times 15 \times 25 \text{ cm}^3$, and a fan was placed at one end of the chamber to transport ions by a free round jet. A dc voltage of $\pm 9 \text{ kV}$ was applied to a tapered single electrode of the ion generator. The generator was designed to suppress the generation of ozone within 0.01 ppm. The small negative ions generated were conveyed by air flow from a hole 3 cm in diameter at a flow rate of $1.6 \times 10^4 \text{ cm}^3 \text{ min}^{-1}$. The air flow formed a free round jet in a wide-open space. The axis of the jet horizontally situated above 1.1 m from the floor. The concentration of small negative ions along the axis of the jet was measured

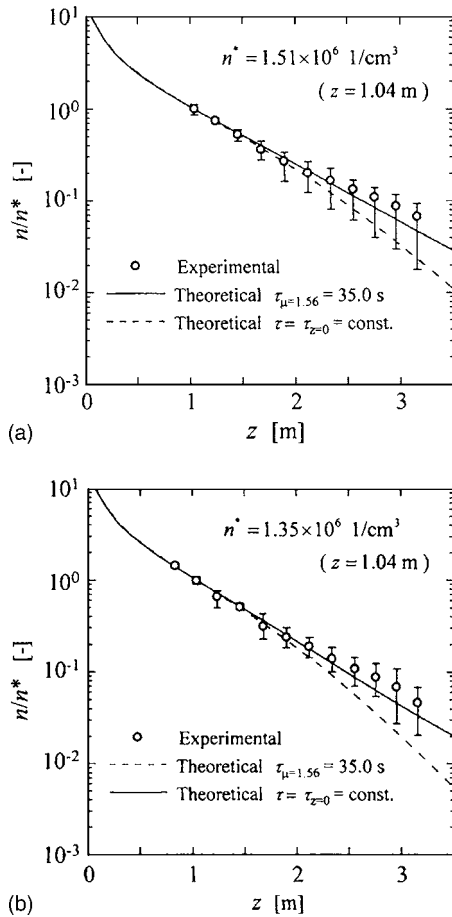


FIG. 3. Concentration of small (a) positive and (b) negative atmospheric ions along the axis of the round free jet.

using a Gerdien-type air ion counter (Universal, IC-1000). The flow rate of air introduced by the counter was $248 \text{ cm}^3 \text{ s}^{-1}$, being negligibly small compared to the flow rate of jet. The measurements were made at a time interval of 5 s, and the average was made from measurements over 6 min, because of the temporal change in concentration showed large variations at low frequencies. The measuring distance ranged from 80 to 320 cm, where the electric field formed between the high-voltage electrode and the air ion counter does not affect the measurements. The temperatures were within a range of $18.1\text{--}24.0 \text{ }^\circ\text{C}$, and the relative humidities were within a range of $31\%\text{--}53\%$.

VI. RESULTS AND DISCUSSION

Figure 3 shows the concentration n of small negative ions in air as a function of the axial distance z of the round free jet. The concentrations are normalized by the measured values at $z=1.04 \text{ m}$. The concentration decreases exponentially with an increase in z , and is correlated well with the solid line, which is calculated from Eq. (17) for i component by assuming that the lifetime of the negative ion of the maximum concentration in spectrum (mobility $\mu = 1.56 \text{ cm}^2 \text{ V}^{-1} \text{ s}^{-1}$) is 35 s. The differential width of the mobility for i component of small ions used to calculate mobility spectra were $0.1 \text{ cm}^2 \text{ V}^{-1} \text{ s}^{-1}$. Also shown by a broken line is the calculation by assuming that the mean lifetime

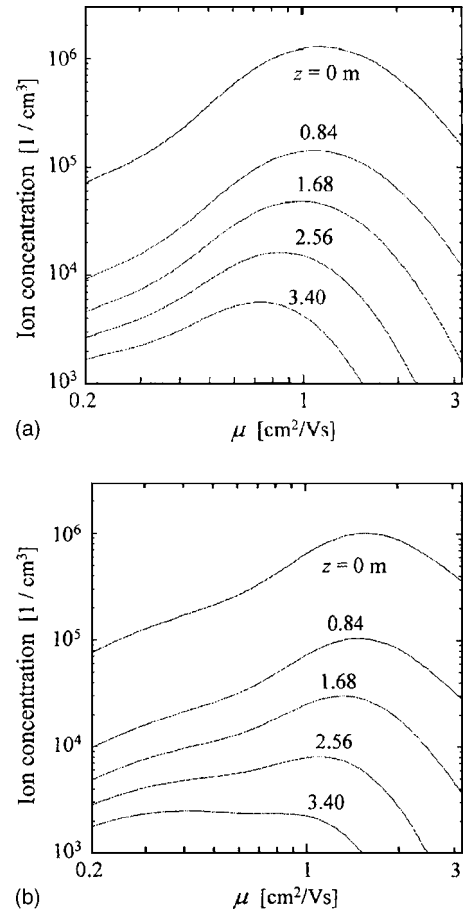


FIG. 4. Calculated mobility spectra of small (a) positive and (b) negative atmospheric ions at five locations.

(30.29 and 36.48 s for negative and positive ions, respectively) obtained at $z=0$ does not change with z . As shown in the previous paper,⁹ the differences between the solid line and broken line are small at $z < 2 \text{ m}$. At z above 2 m , however, the deviation increases with increasing z , indicating that the mean lifetime increases with flowing downstream.

Figure 4 shows the calculated mobility spectra of small ions at five locations. They were obtained from the theoretical calculation of the concentration n_i . The spectra change with decreasing concentration; the fraction of higher mobility rapidly decreases compared with that of lower mobility, because of the shorter lifetime. Figure 5 shows the mean lifetime τ_{ave} as a function of axial distance z of the free round jet. It is obtained by substituting the measured concentration into Eq. (23). The rather large error bars in the results are attributable to differentiation of nonsmoothing data in the calculations. Also shown in this figure is the theoretical mean lifetime, which is obtained by Eqs. (20) and (21) and theoretical concentration Eq. (17). Agreements with the measurements are fairly well, indicating that the mean lifetime increases with increasing axial distance z . In particular, the increase is apparent at a distance above 2 m . Thus the mobility spectra of small ions shifts to a lower value in a non-equilibrium condition, where a large number of small ions are artificially generated at one source in space and connected by air flow.

For further detailed analysis of the change in mobility

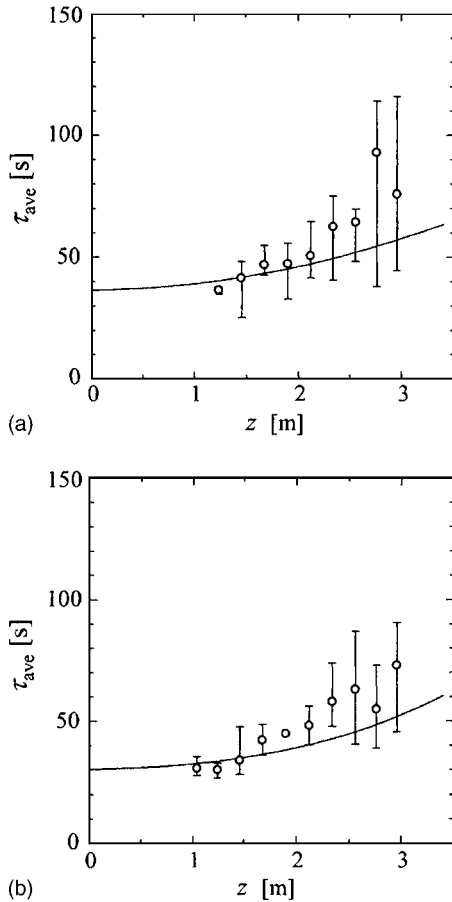


FIG. 5. Mean lifetime of small (a) positive and (b) negative atmospheric ions along the axis of the round free jet.

spectra, the electrostatic repulsion of the ion should be taken into account in the analysis of the experimental concentration distribution. The electrostatic repulsion of the ion may not be negligibly small at the upstream near the source where high-concentration small ions are artificially generated by the generator. In addition, the experimental mobility spectra should be used in the discussion, because the reported mobility spectra of artificially generated ions show some differences from that of the naturally generated small ions. They depend on the method of the generation.

VII. CONVECTIVE TRANSFER OF SMALL NEGATIVE IONS FROM MOUTH TO LUNGS BY BREATHING

In the recent paper,⁹ a simple pipe-flow model is used to calculate the convective transport of ions in a human body from the mouth to the lungs by breathing. The air flow during inspiration through the trachea from the mouth to the lungs is approximated as flow at constant velocity through a straight circular pipe with a rigid wall. For simplicity in calculation, the concentration distribution across the trachea is approximated as flat and the transfer of ions to the trachea wall by radial diffusion is expressed using the mass-transfer coefficient. Thus, the convective transport of i component with dissipation by collisions with large particles and the trachea wall is expressed as

TABLE I. Characteristics of breathing and air.

Representative diameter of trachea, d	2.5 cm
Length of trachea from mouth to lungs, L	25 cm
Volume of inspiration	300 cm ³
Frequency of breathing	18 min ⁻¹
Time-averaged volumetric flow rate of inspiration	180 cm ³ s ⁻¹
Time-averaged velocity of inspiration	36.7 cm s ⁻¹
Density of air (at 20 °C)	1.286 × 10 ⁻³ g cm ⁻³
Viscosity of air (at 20 °C)	1.80 × 10 ⁻⁴ g cm ⁻¹ s ⁻¹
(Re=655; Sc=3.26; Sh _{av} =9.69)	

$$n_i/n_{i0} = \exp[-(4k_{av}/d + \beta_i N)z/V], \quad (24)$$

where V , k_{av} , d , and z represent the velocity of air, space-averaged mass-transfer coefficient of the ion, the diameter of the trachea, and the axial distance. Table I lists the characteristics of human breathing¹⁸ and air. Under the assumption that the period of inspiration is equal to that of expiration, the time-averaged volumetric flow rate was calculated by multiplying the air volume inspired by twice the frequency of breathing. The space-averaged mass-transfer coefficient k_{av} was obtained from the correlation for the space-averaged Sherwood number Sh_{av} in a laminar pipe flow,

$$Sh_{av} \equiv k_{av}d/D = 1.62(\text{Re} \text{ Sc } d/L)^{1/3}. \quad (25)$$

Substituting these values into Eq. (24) yields $n/n_0=0.813$ and 0.835 for negative and positive ions, respectively. This fact indicates that most of the small atmospheric ions entering from the mouth reach the lungs. This is attributable to the high convective velocity, which overcomes the rapid dissipation that occurs in windless air. Figure 6 shows the mobility spectra of negative ions at mouth and lungs. The spectra show a little shift to smaller mobility. It is attributable to the fact that the higher the mobility the faster the dissipation by collisions with large particles and the trachea wall becomes.

VIII. CONCLUSIONS

There occurs no change in mobility spectra for the molecular diffusion in windless air, because both coefficients of adhesion and diffusion are proportional to the mobility. On the other hand, the mobility spectra of ions change during the convections due to the inverse proportionality of the lifetime to the mobility of ions.

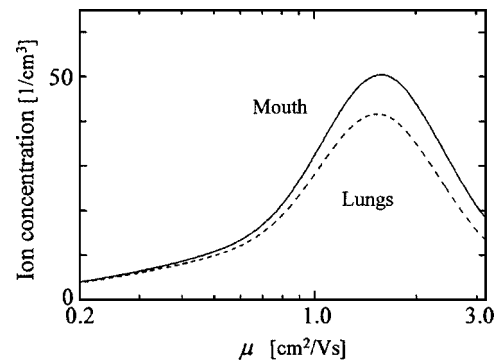


FIG. 6. Mobility spectra of small negative atmospheric ions at mouth and lungs.

ACKNOWLEDGMENTS

The authors would like to thank Dr. K. Nagato of Kochi National College of Technology for his support on this study and Y. Komaki of Eco Holistic Inc. for providing the ion generator.

- ¹U. Hörrak, J. Salm, and H. Tammet, *J. Geophys. Res.* **105**, 9291 (2000).
²W. Gringel, J. M. Rosen, and D. J. Hoffmann, *The Earth's Electrical Environment*, Studies in Geophysics (National Academic, Washington, DC, 1986), p. 166.
³R. G. Harrison and K. S. Carslaw, *Rev. Geophys.* **41**, 1012 (2003).
⁴J. Bricard and J. Pradel, in *Aerosol Science*, edited by C. N. Davies (Academic, London, 1966), p. 87.
⁵K. Nagato and T. Ogawa, *Planet. Space Sci.* **36**, 163 (1988).
⁶K. Nagato and T. Ogawa, *J. Geophys. Res.* **103**, 13917 (1998).
⁷K. Nagato, *Proc. Inst. Electrostat. Jpn.* **23**, 37 (1999).

- ⁸M. Misaki, *Kisho Kenkyu Noto* **130**, 685 (1976) (in Japanese).
⁹T. Maruyama and T. Katayama, *J. Appl. Phys.* **94**, 7365 (2003).
¹⁰H. Israël, *Atmosphärische Elektrizität* (I. Akademische Verlagsgesellschaft, Leipzig, 1957).
¹¹J. A. Chalmer, *Atmospheric Electricity*, 2nd ed. (Pergamon, Oxford, 1957).
¹²J. Bricard, *J. Geophys. Res.* **54**, 39 (1949).
¹³J. Bricard, *Geofis. Pura Appl.* **51**, 237 (1962).
¹⁴M. Misaki, *Kisho Kenkyu Noto* **142**, 1 (1981) (in Japanese).
¹⁵L. B. Loeb, *Basic Processes of Gaseous Electronics* (University of California Press, Berkeley, 1960).
¹⁶R. B. Bird, W. E. Stewart, and E. N. Lightfoot, *Transport Phenomena* (Wiley, New York, 1960).
¹⁷L. L. Simpson, in *Turbulence in Mixing Operation*, edited by R. S. Brodkey (Academic, New York, 1975), p. 277.
¹⁸J. K. Inglis, *A Textbook of Human Biology*, 3rd ed. (Butterworth Heine-
mann, London, 1988).